

Observation of three superconducting transitions in the pressurized CDW-bearing compound TaTe₂

Jing Guo^{1,6}, Cheng Huang^{1,5}, Huixia Luo,² Huaixin Yang,¹ Linlin Wei,¹ Shu Cai,¹ Yazhou Zhou,¹ Hengcan Zhao,¹ Xiaodong Li^{1,3}, Yanchun Li,³ Ke Yang,⁴ Aiguo Li,⁴ Peijie Sun,¹ Jianqi Li,¹ Qi Wu,¹ Robert J. Cava,² and Liling Sun^{1,5,6,*}

¹*Institute of Physics, Chinese Academy of Sciences, Beijing 100190, China*

²*Department of Chemistry, Princeton University, Princeton, New Jersey 08544, USA*

³*Institute of High Energy Physics, Chinese Academy of Sciences, Beijing 100049, China*

⁴*Shanghai Synchrotron Radiation Facilities, Shanghai Institute of Applied Physics, Chinese Academy of Sciences, Shanghai 201204, China*

⁵*University of Chinese Academy of Sciences, Beijing 100190, China*

⁶*Songshan Lake Materials Laboratory, Dongguan, Guangdong 523808, China*



(Received 15 December 2021; revised 12 April 2022; accepted 22 April 2022; published 9 May 2022)

Transition metal dichalcogenides host a wide variety of lattice and electronic structures, as well as corresponding exotic physical properties, especially under certain tuning conditions. Here, we report the observation of pressure-induced three superconducting transitions in TaTe₂, a charge density wave (CDW)-bearing layered transition-metal dichalcogenide that is metallic but not superconducting at ambient pressure. We find that its CDW state can be easily suppressed upon increasing pressure up to ~1 GPa. A superconducting state then emerges from the suppressed CDW state and persists to the pressure about 7 GPa. Unexpectedly, another superconducting state appears at ~11 GPa within the same monoclinic (M) structure of its ambient-pressure one. Upon further compression to 21 GPa, a third superconducting state with higher T_c appears from a high-pressure (HP) phase. Our experimental results suggest that the pressure-induced three superconducting transitions in TaTe₂ are, respectively, driven by the suppression of the CDW state, the change of the β angle in the M phase and the transition of M-to-HP phase. These results demonstrate not only the versatile nature of this correlated electron system, but also the first experimental example that shows the pressure-induced evolution from a CDW state to three superconducting states driven by different mechanisms.

DOI: [10.1103/PhysRevMaterials.6.L051801](https://doi.org/10.1103/PhysRevMaterials.6.L051801)

In layered transition metal dichalcogenides, a charge density wave (CDW) is frequently observed, appearing as a periodic modulation of the electronic charge density [1–6]. Through chemical doping or under applied pressure, many of these compounds show a competition between the CDW ordered state and superconductivity [1,6–11], similar to the behavior that is observed in unconventional superconductors whose superconductivity resides near the boundary of an ordered magnetic state. There are many examples that demonstrate the close connection between superconductivity and ordered state, such as the magnetic orders in iron-based superconductors, the heavy Fermion superconductors, and the copper oxide superconductors [12–15]. The same is true for the connection between superconductivity and CDW order.

In this study, we report a case, finding pressure-induced three superconducting transitions in the nonsuperconducting CDW-bearing compound TaTe₂, revealed by complementary measurements of *in situ* high pressure electrical resistance, ac susceptibility, Hall coefficient, angle dispersive x-ray diffraction (XRD), and transmission electron microscopy (TEM).

The high-quality single crystals were synthesized by the chemical vapor transport method, using iodine as a transport

agent [16]. Pressure was generated by two types of high-pressure cells, piston-cylinder and diamond anvil cell, for the low and high pressure measurements. In the low-pressure measurements (up to 2.11 GPa), 7373 oil was used as pressure transmitting medium and pressure was determined by the pressure dependence of T_c of Pb [17] that was placed together with the sample in a Teflon capsule. For the high-pressure measurements, up to ~40 GPa, diamond anvils with 300 μm flats were employed, and NaCl powder was used as the pressure transmitting medium to obtain a quasihydrostatic pressure environment. The sample sizes for the low and high pressure measurements were 2 mm \times 1 mm \times 0.2 mm and 60 μm \times 60 μm \times 5 μm , respectively. High-pressure electrical resistance and Hall coefficient measurements were carried out using a standard four-probe technique and the Van der Pauw method [18–20]. High-pressure alternating current (ac) susceptibility measurements were conducted using homemade primary/secondary-compensated coils around a diamond anvil [18,21]. High-pressure x-ray diffraction (XRD) measurements were carried out at beamline 4W2 at the Beijing Synchrotron Radiation Facility and at beamline 15U at the Shanghai Synchrotron Radiation Facility. A monochromatic x-ray beam with a wavelength of 0.6199 Å was used and silicon oil was employed as a pressure-transmitting medium. The pressure for all measurements, in a diamond anvil cell, was determined by the ruby fluorescence method [22]. Ambient-pressure TEM observations were performed on a JEOL 2100F transmission

*Correspondence and requests for materials should be addressed to: llsun@iphy.ac.cn

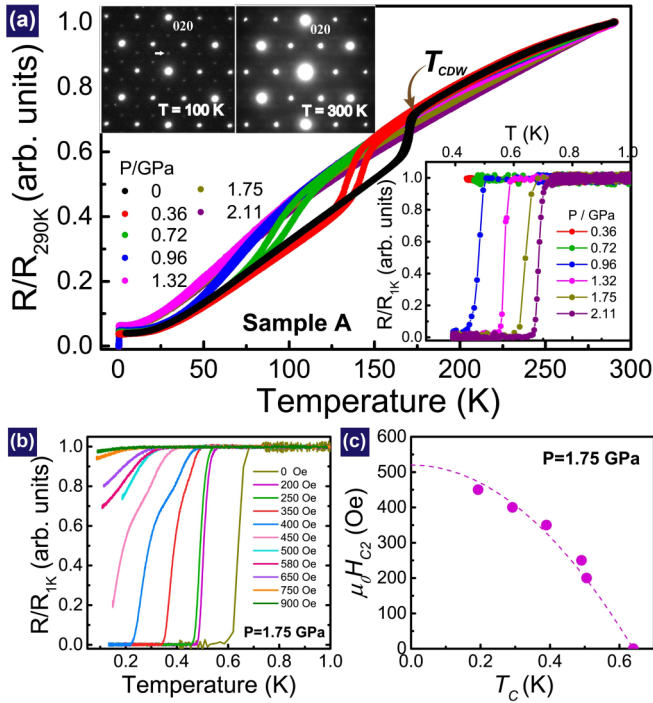


FIG. 1. Characterizations for TaTe₂ single crystal (a) The normalized resistance as a function of temperature at pressures below 2.11 GPa. The upper left insets display electron-diffraction patterns taken along the $[-101]$ zone axis direction at 100 and 300 K, respectively; the superstructure due to the existence of the CDW state at low temperature is indicated by an arrow. The lower right inset displays an enlarged view of the normalized resistance versus temperature below 1 K. (b) The temperature dependence of the normalized resistance under different magnetic fields at 1.75 GPa. (c) H_{C2} as a function of temperature. The dashed line represents the Ginzburg-Landau (GL) fits.

electron microscope equipped with a low-temperature sample holder.

First, we performed *in situ* resistance measurements on the TaTe₂ sample in the low pressure range by using a piston-cylinder pressure cell. Figure 1(a) shows the electrical resistance as a function of temperature down to ~ 0.4 K at different pressures up to 2.11 GPa. It is seen that the resistance of the ambient-pressure sample exhibits an anomaly at ~ 175 K, due to the CDW transition [23–26]. To better specify this resistance anomaly, we carried out TEM measurements at ambient-pressure at 300 and 100 K, respectively. The electron-diffraction patterns taken along the $[-101]$ direction at two different temperatures are shown in the inset of Fig. 1(a). It is seen that a new set of electron-diffraction reflections, which is not present at 300 K, appears in reciprocal space at 100 K, signaling the existence of the CDW order. To know the evolution of the CDW ordered state with pressure, we applied high pressure on the TaTe₂ sample and measured the temperature dependence of the resistance in a warming and cooling cycle at different pressures [Fig. 1(a) and Fig. S1 in Ref. [27] Supplementary Material (SM)]. A thermal hysteresis in resistivity is observed (Fig. S1 in Ref. [27]), which is considered to be a typical feature of the CDW transition [23,26]. We found that the formation temperature of the CDW

state, T_{CDW} , decreases with increasing pressure and then is undetectable at ~ 1.32 GPa [Fig. 1(a)]. Moreover, the sample shows a sharp resistance drop at ~ 0.5 K under a pressure of about 0.96 GPa, which is close to the boundary of the suppressed CDW state. A zero-resistance state is achieved at ~ 0.4 K, indicative of a superconducting transition [as shown in the lower right inset of Fig. 1(a)]. The onset temperature of the superconducting transition (T_c) increases with further compression up to 2.11 GPa, the maximum pressure of this experimental run. To further characterize the observed superconducting behavior in the pressurized TaTe₂, we applied magnetic fields for TaTe₂ subjected to 1.75 GPa [Fig. 1(b)]. It is found that its resistance drop shifts to lower temperature with increasing magnetic field and completely vanishes at ~ 900 Oe. These results indicate that the pressure-induced resistance drop is associated with a superconducting transition. We extract the field dependence of midpoint T_c for TaTe₂ at 1.75 GPa and estimate the upper critical magnetic field at zero temperature to be about ~ 520 Oe [Fig. 1(c)].

To investigate the evolution of the observed superconducting state under higher pressure, we carried out high-pressure measurements on the TaTe₂ samples in a diamond anvil cell. As shown in Fig. 2(a), the superconducting transition with a zero-resistance state is seen at 2.1 GPa and the T_c value slightly shifts to higher temperature at 3.6 GPa. Upon increasing pressure to 5.9 GPa, the sample loses its zero resistance. At 8.3 GPa, the resistance drop is not observable at temperature down to ~ 0.3 K, revealing that the superconducting state is suppressed by high pressure. Interestingly, when we applied pressure up to 11.5 GPa, the resistance drop reemerges and zero resistance is observed at ~ 0.5 K, indicating that a new superconducting state appears [Fig. 2(b)]. The onset transition temperature of this new superconducting state increases with elevating pressure, but the transition becomes broad starting at ~ 15 GPa. Its T_c value shifts to high temperature slightly upon compression to 24 GPa [Fig. 2(c)]. At ~ 27.5 GPa, unexpectedly, we found another resistance drop, at ~ 3.5 K. The onset temperature of this resistance drop shifts slightly to higher temperature with increasing pressure [Fig. 2(c)]. We repeated the measurements with new samples in different experiments, and found that the results were reproducible [Figs. 2(d)–2(f) and Fig. S2 in Ref. [27]]. To characterize the superconducting transition in the pressure range of 10–22 GPa and 22–40.5 GPa, we applied a magnetic field on TaTe₂ subjected to 13.6 and 40.5 GPa [Figs. 2(g) and Fig. S3a], and found that the resistance drop shifts to lower temperature with increasing magnetic field and the estimated upper critical magnetic fields at zero temperature are ~ 680 Oe at 13.6 GPa, and ~ 2850 Oe at 40.5 GPa. The observation of the different upper critical magnetic fields in the second and third superconducting states implies that they may have different natures.

In order to confirm these pressure-induced superconducting transitions, high-pressure ac susceptibility measurements were performed in a diamond anvil cell up to 32.6 GPa. The onset temperature of the diamagnetism was observed at 0.5, 0.53, and 0.7 K at pressures of 2.9, 15.3, and 24.5 GPa, respectively [Fig. 2(i)]. All these results indicate that the pressure-induced resistance drops are attributable to the superconducting transitions of bulk superconductivity. We did not observe a diamagnetic signal from our ac susceptibility mea-

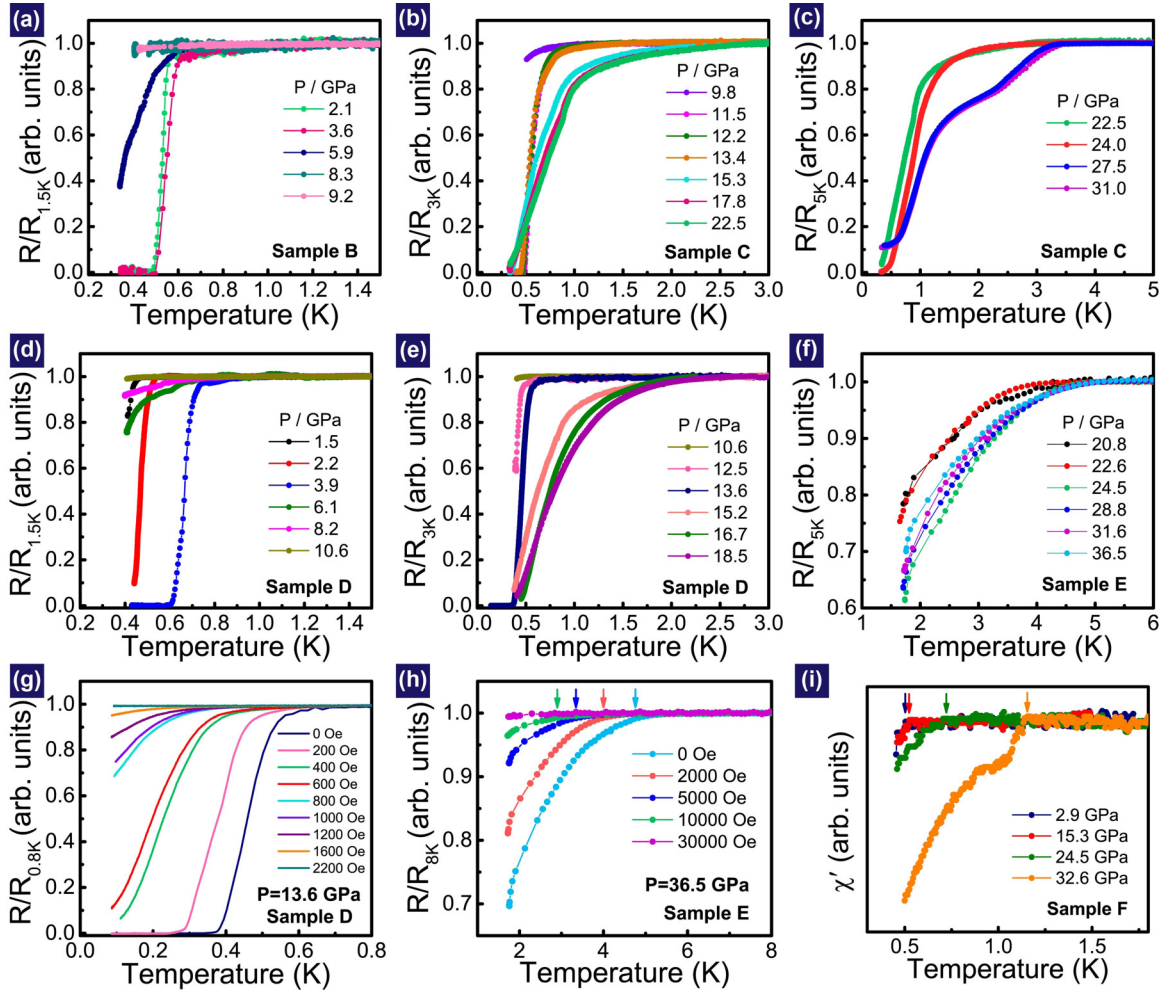


FIG. 2. Electronic resistance and diamagnetism measurements for pressurized TaTe₂ (a) The normalized resistance as a function of temperature for the sample B in the pressure range of 2.1–9.2 GPa. (b),(c) for the sample C in the pressure range of 9.8–22.5 GPa and 22.5–31.0 GPa, respectively. (d),(e) for the sample D obtained in the pressure range of 1.5–10.6 GPa and 10.6–18.5 GPa, respectively. (f) for the sample E in the pressures range of 20.8–36.5 GPa. (g),(h) The temperature dependence of the normalized resistance under different magnetic fields at 13.6 GPa for the sample D and at 36.5 GPa for the sample E. (i) The real part of the alternating-current (ac) susceptibility (χ') as a function of temperature for the sample F at different pressures. The arrows denote the temperatures of the superconducting transition.

measurements at the temperature near the onset of the resistance drop in the pressure range that the third superconducting state exists, implying that the superconductivity of the third superconducting state is likely a filament one [Fig. 2(i)]. While the diamagnetism observed at 1.15 K and 32.6 GPa should be from the second superconducting state that coexists with the third one at this pressure (see high-pressure XRD data below).

High pressure synchrotron XRD measurements were performed at the two Synchrotron Radiation Facilities to clarify whether the observed superconducting transitions in pressurized TaTe₂ are related to the structure phase transitions (Fig. 3 and S4 in Ref. [27]). The XRD patterns collected at the Beijing Synchrotron Radiation Facility are displayed in Fig. 3(a). It is found that all peaks can be indexed well with the monoclinic phase in the $C2/m$ space group below 21 GPa, indicating that its ambient-pressure phase of TaTe₂ is stable below 21 GPa. However, a new peak appears at ~ 13 degrees when pressure is increased to 21.3 GPa [Fig. 3(a)] and 23 GPa (Fig. S4 in Ref. [27]), and its intensity increases with pressure, indicating that the pressure induces a new structural phase

transition. Since the new phase cannot be exactly refined by a single peak, here we have to define it as the high pressure (HP) phase. We found that this HP phase coexists with the ambient-pressure M phase under pressure up to 40 GPa (Fig. S4 in Ref. [27]). Based on our XRD results, we extract the pressure dependence of lattice parameters and volume [Figs. 3(b)–3(d)]. It is seen that the pressure-dependent lattice constants and volumes determined from the two independent diffraction measurements at the two different synchrotron x-ray sources are in good agreement with each other, and the lattice constants and volume do not exhibit any discontinuities with increasing pressure to 40 GPa. These results demonstrate that the ambient-pressure M phase is stable under pressure to 40 GPa, which indicates that the HP phase is developed from the matrix of its ambient-pressure M phase.

We summarize the high-pressure transport results and structure information for TaTe₂ in Fig. 4(a). It is found that the first superconducting (SC-I) state emerges from a suppressed CDW state, vanishes at ~ 7 GPa, and that the second superconducting (SC-II) state appears at ~ 11 GPa, followed by

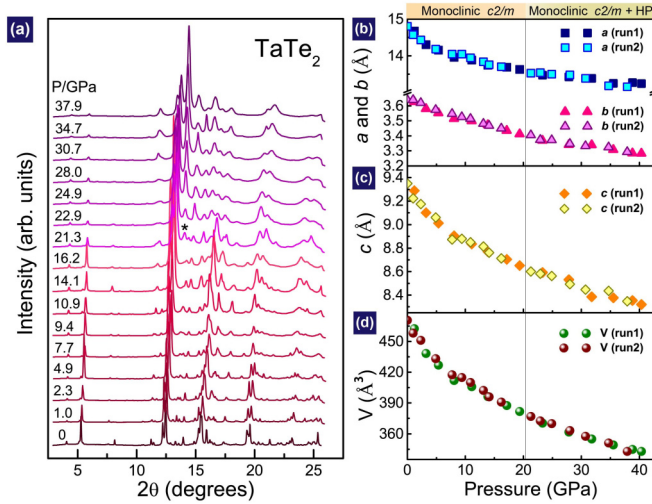


FIG. 3. Structural characterization of TaTe₂ (a) The x-ray diffraction patterns obtained at different pressures. A new peak beginning at ~ 21 GPa is observed, indicated by a star, suggesting that at this pressure a new structure phase emerges on the matrix of the monoclinic phase. (b)–(d) The pressure dependence of the lattice constants (*a*, *b*, and *c*) and unit cell volume (*V*) obtained from two independent measurements at two different synchrotron sources.

the appearance of the third superconducting (SC-III) state at ~ 21 GPa. The crystal structure of the SC-I state and the SC-II state reside in the ambient-pressure M phase, while the SC-III state is likely to be within the HP phase, because the SC-III phase appears just when the HP phase forms at ~ 21 GPa and the T_c value of the TaTe₂ sample shows a jump at ~ 21 GPa, which is often seen in many of the phase-transition-induced superconducting state [28]. Therefore, we propose that the formation of the HP phase is responsible for the emergence of SC-III phase. Moreover, our proposal about that superconductivity of the SC-III state may be a filamentlike one is also supported by our XRD results, in which only one XRD peak of the HP phase appears on the matrix of the M phase within the pressure range it exists. Certainly, the nature of the SC-III state calls for further investigations both from experimental and theoretical sides.

To understand the evolution of the pressure-induced multiple superconducting transitions from the CDW ordered state, we performed high-pressure Hall resistance and magnetoresistance (MR) measurements on the TaTe₂ sample by sweeping the magnetic field perpendicular to the *ab* plane at two temperatures (4 and 10 K) and various pressures. The pressure dependence of the Hall coefficient (R_H) and the MR% (MR is defined as $[(R(7T) - R(0T))/R(0T)] \times 100\%$) are illustrated in Fig. 4(b) and the SM. At ambient pressure, the Hall coefficient (R_H) displays a positive sign both at 4 and 10 K, implying that hole-carriers are dominant. Meanwhile, the sample displays a positive magnetoresistance effect (MR% = 62). Within the pressure range of the CDW ordered state, R_H and MR% dramatically decrease with increasing pressure, suggesting that the role of electron carriers is enhanced by applying pressure. At ~ 1 GPa, the SC-I state emerges from the suppressed CDW order state, in accordance with the common picture seen in layered transition metal

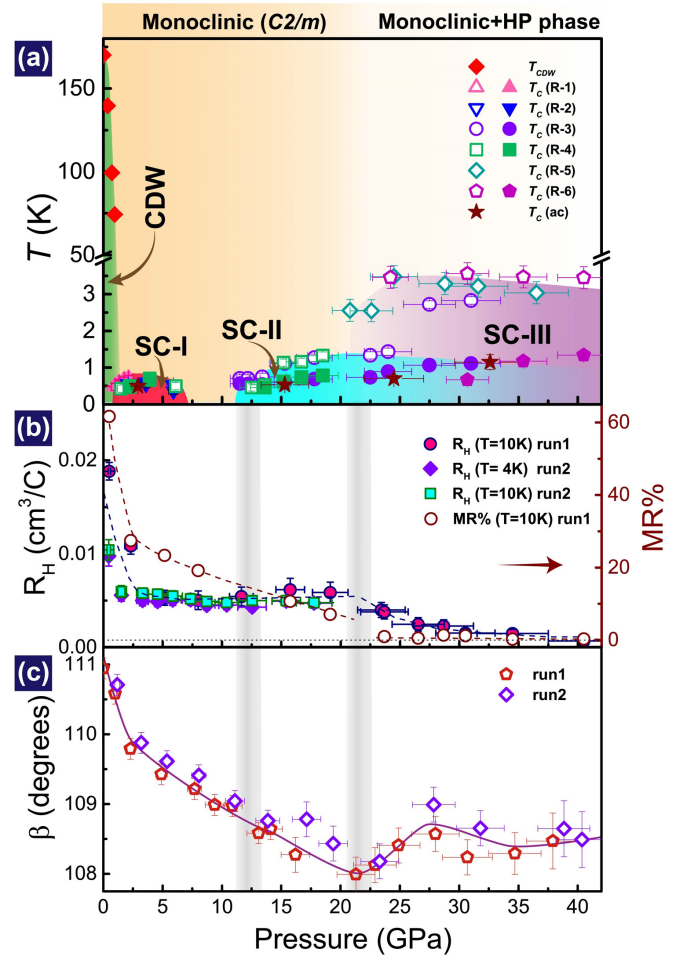


FIG. 4. Summary of the experimental observations on TaTe₂ (a) Pressure-temperature phase diagram combined with structure information for TaTe₂. T_{CDW} represents the formation temperature of the CDW state. $T_c(R)$ represents the superconducting transition temperature determined by the resistance measurements. The open and solid symbols represent the superconducting transition temperatures that were defined as temperatures where the resistance falls to 90% and 50% of the normal state value, respectively. $T_c(ac)$ represents the superconducting transition temperature determined by ac susceptibility measurements. (b) The pressure dependent Hall coefficient (R_H) measured at 4 and 10 K (left axis). The magnetoresistance (MR) as a function of pressure measured at 10 K (right axis), here $MR\% = [R(7T) - R(0T)]/R(0T) \times 100\%$. (c) The β angle of the monoclinic structure as a function of pressure.

dichalcogenides [6,8,9,29], implying that the superconducting electrons in the SC-I state are released from the CDW state. The evolution of T_c with pressure in SC-I state forms a dome-like shape with a maximum T_c of 0.7 K at ~ 3.5 GPa. While, in the pressure range of ~ 11 – 21 GPa, the SC-II state presents without a structural phase transition. We found that the values of the Hall coefficient R_H at 4 and 10 K remain nearly constant in the pressure range where the SC-II state exists, suggesting that the SC-II state develops from a semimetal state [30]. To further investigate the origin the SC-II state, we extracted the pressure dependence of the angle β that represents the lattice deformation degree of the monoclinic phase and found that

the value of the β angle is $\sim 111^\circ$ at ambient pressure, and it is reduced with increasing pressure, reaches to 108.5° at ~ 12.5 GPa where the SC-II state presents. We suggest that reducing β angle by $\sim 2.5^\circ$ and more can induce the appearance of the SC-II state. At ~ 21 GPa, the β angle starts to show an increase with pressure, which is likely associated with the presence of the HP phase developed from the matrix of the monoclinic phase.

We propose that the semimetal state may be associated with the peculiar positive magnetoresistance state that is observed [Fig. 4(b)]. Such behavior is reminiscent of what has been seen in the pressurized Weyl semimetal WTe_2 , which displays a large positive magnetoresistance at ambient pressure [31]. High pressure studies on WTe_2 found that as long as the positive magnetoresistance effect prevails, no superconductivity is present, i.e., the superconductivity only appears when the positive magnetoresistance effect is completely suppressed [19,32]. For pressurized TaTe_2 , we found that the SC-III state with higher superconducting transition temperature emerges at pressures above ~ 21 GPa, a pressure where a new structure sets in (Fig. 3), meanwhile, the positive magnetoresistance suddenly disappears and the Hall coefficient shows a drop starting at ~ 21 GPa [Fig. 4(b)]. Based on these experimental results, we propose that the HP phase emerging at ~ 21 GPa manifests a topology change of the Fermi surface, which in turn tips the electronic structure at the Fermi level in favor of superconductivity.

In summary, we report the observation of pressure-induced three superconducting transitions in the CDW-bearing

compound TaTe_2 . We propose the possible reasons for these three superconducting states as follows: the suppression of the CDW ordered state and the enhancement of superconducting carrier density lead to the appearance of the SC-I state; the critical β angle of the M phase drives the emergence of the SC-II state; and the pressure-induced structural phase transition gives rise to the development of the SC-III state. To the best of our knowledge, this is the only experimental example that three different superconducting transitions can be tuned out by pressure from one compound with a homogenous lattice structure. These results are expected to shed new insight on the underlying superconducting mechanisms in the correlated electron systems of the transition metal ditellurides, and even in the other unconventional superconducting compounds.

This work in China was supported by the NSF of China (Grants No. U2032214, No. 12122414, No. 12104487, and No. 12004419), the National Key Research and Development Program of China (Grants No. 2017YFA0302900 and No. 2017YFA0303103), and the Strategic Priority Research Program (B) of the Chinese Academy of Sciences (Grant No. XDB25000000). We acknowledge the support from the Users with Excellence Program of Hefei Science Center CAS (2020HSC-UE015). Part of the work is supported by the Synergic Extreme Condition User System. J. G. is grateful for support from the Youth Innovation Promotion Association of the CAS (2019008). The work at Princeton was supported by the U.S. Department of Energy, Division of Basic Energy Sciences, Grant No. DE-FG02-98ER45706.

-
- [1] J. A. Wilson and A. D. Yoffe, *Adv. Phys.* **18**, 193 (1969).
 - [2] J. A. Wilson, F. J. Di Salvo, and S. Mahajan, *Adv. Phys.* **24**, 117 (1975).
 - [3] F. J. Di Salvo, D. E. Moncton, and J. V. Waszczak, *Phys. Rev. B* **14**, 4321 (1976).
 - [4] S. J. Kim, S. J. Park, I. C. Jeon, C. Kim, C. Pyun, and K. A. Yee, *J. Phys. Chem. Solids* **58**, 659 (1997).
 - [5] T. Kasuya, M. H. Jung, and T. Takabatake, *J. Magn. Magn. Mater.* **220**, 235 (2000).
 - [6] E. Morosan, H. W. Zandbergen, B. S. Dennis, J. W. G. Bos, Y. Onose, T. Klimczuk, A. P. Ramirez, N. P. Ong, and R. J. Cava, *Nat. Phys.* **2**, 544 (2006).
 - [7] G. Grüner, *Rev. Mod. Phys.* **60**, 1129 (1988).
 - [8] B. Sipos, A. F. Kusmartseva, A. Akrap, H. Berger, L. Forro, and E. Tutis, *Nat. Mater.* **7**, 960 (2008).
 - [9] T. Lin, X. J. Wang, X. Chen, X. B. Liu, X. Luo, X. Li, X. L. Jing, Q. Dong, B. Liu, H. Y. Liu, Q. J. Li, X. B. Zhu, and B. B. Liu, *Inorg. Chem.* **60**, 11385 (2021).
 - [10] K. Yamaya, M. Yoneda, S. Yasuzuka, Y. Okajima, and S. Tanda, *J. Phys.: Condens. Matter* **14**, 10767 (2002).
 - [11] B. S. Wang, Y. Liu, K. Ishigaki, K. Matsubayashi, J. G. Cheng, W. J. Lu, Y. P. Sun, and Y. Uwatoko, *Phys. Rev. B* **95**, 220501(R) (2017).
 - [12] N. D. Mathur, F. M. Grosche, S. R. Julian, I. R. Walker, D. M. Freye, R. K. W. Haselwimmer, and G. G. Lonzarich, *Nature (London)* **394**, 39 (1998).
 - [13] P. C. Canfield and S. L. Bud'ko, *Ann. Rev. Condens. Matter Phys.* **1**, 27 (2010).
 - [14] J. M. Tranquada, B. J. Sternlieb, J. D. Axe, Y. Nakamura, and S. Uchida, *Nature (London)* **375**, 561 (1995).
 - [15] B. Keimer, S. A. Kivelson, M. R. Norman, S. Uchida, and J. Zaanen, *Nature (London)* **518**, 179 (2015).
 - [16] H. X. Luo, W. W. Xie, J. Tao, H. Inoue, A. Gyenis, J. W. Krizan, A. Yazdani, Y. M. Zhu, and R. J. Cava, *Proc. Natl Acad. Sci.* **112**, E1174 (2015).
 - [17] A. Eiling and J. S. Schilling, *J. Phys. F* **11**, 623 (1981).
 - [18] L. L. Sun, X. J. Chen, J. Guo, P. W. Gao, Q. Z. Huang, H. D. Wang, M. H. Fang, X. L. Chen, G. F. Chen, Q. Wu, C. Zhang, D. C. Gu, X. L. Dong, L. Wang, K. Yang, A. G. Li, X. Dai, H. K. Mao, and Z. X. Zhao, *Nature (London)* **483**, 67 (2012).
 - [19] D. F. Kang, Y. Z. Zhou, W. Yi, C. L. Yang, J. Guo, Y. G. Shi, S. Zhang, Z. Wang, C. Zhang, S. Jiang, A. G. Li, K. Yang, Q. Wu, G. M. Zhang, L. L. Sun, and Z. X. Zhao, *Nat. Commun.* **6**, 7804 (2015).
 - [20] L. J. Van der Pauw, *Philips. Tech. Rev.* **20**, 220 (1958).
 - [21] M. Debossai, J. J. Hamlin, and J. S. Schilling, *Phys. Rev. B* **78**, 064519 (2008).
 - [22] H. K. Mao, J. Xu, and P. M. Bell, *J. Geophys. Res.* **91**, 4673 (1986).
 - [23] T. Söregel, J. Nuss, U. Wedig, R. K. Kremer, and M. Jansen, *Mater. Res. Bull.* **41**, 987 (2006).
 - [24] Y. Liu, W. J. Lu, D. F. Shao, L. Zu, X. C. Kan, W. H. Song, and Y. P. Sun, *EPL* **109**, 17003 (2015).

- [25] J. G. Feng, A. Tan, S. Wagner, J. Y. Liu, Z. Q. Mao, X. L. Ke, and P. P. Zhang, *App. Phys. Lett.* **109**, 021901 (2016).
- [26] H. X. Chen, Z. L. Li, L. W. Guo, and X. L. Chen, *EPL* **117**, 27009 (2017).
- [27] See Supplemental Material at <http://link.aps.org/supplemental/10.1103/PhysRevMaterials.6.L051801> for details on pressure effects on CDW and upper critical field, extended high-pressure resistance and XRD measurements, high-pressure Hall coefficient, and magnetic resistance measurements.
- [28] S. Cai, S. K. Kushwaha, J. Guo, V. A. Sidorov, C. C. Le, Y. Z. Zhou, H. H. Wang, G. C. Lin, X. D. Li, Y. C. Li, K. Yang, A. G. Li, Q. Wu, J. P. Hu, Robert J. Cava, and L. L. Sun, *Phys. Rev. Materials* **2**, 114203 (2018).
- [29] A. F. Kusmartseva, B. Sipos, H. Berger, L. Forro, and E. Tutis, *Phys. Rev. Lett.* **103**, 236401 (2009).
- [30] Y. Z. Zhou, D. J. Kim, P. F. S. Rosa, Q. Wu, J. Guo, S. Zhang, Z. Wang, D. F. Kang, W. Yi, Y. C. Li, X. D. Li, J. Liu, P. Q. Duan, M. Zi, X. J. Wei, Z. Jiang, Y. Y. Huang, Y. F. Yang, Z. Fisk, L. L. Sun, and Z. X. Zhao, *Phys. Rev. B* **92**, 241118(R) (2015).
- [31] M. N. Ali, J. Xiong, S. Flynn, J. Tao, Q. D. Gibson, L. M. Schoop, T. Liang, N. Haldolaarachchige, M. Hirschberger, N. P. Ong, and R. J. Cava, *Nature (London)* **514**, 205 (2014).
- [32] X.-C. Pan, X. Chen, H. Liu, Y. Feng, Z. Wei, Y. Zhou, Z. Chi, L. Pi, F. Yen, F. Song, X. Wan, Z. Yang, B. Wang, G. Wang, and Y. Zhang, *Nat. Commun.* **6**, 7805 (2015).